# Fe-N-Doped Hierarchical Mesoporous Carbon Nanomaterials as Efficient Catalysts for Oxygen Reduction in Both Acidic and Alkaline Media

Rongmin Dun,[a,b] Menggeng Hao,[a,b] Yumiao Su[a] and Wenmu Li*[a]

[a.] Key Laboratory of Optoelectronic Materials Chemistry and Physics, Fujian Institute of Research on the Structure of Matter, Chinese Academy of Sciences, Fuzhou 350002, China E-mail: liwm@fjirsm.ac.cn

[b.] University of Chinese Academy of Sciences, Beijing 100049, China

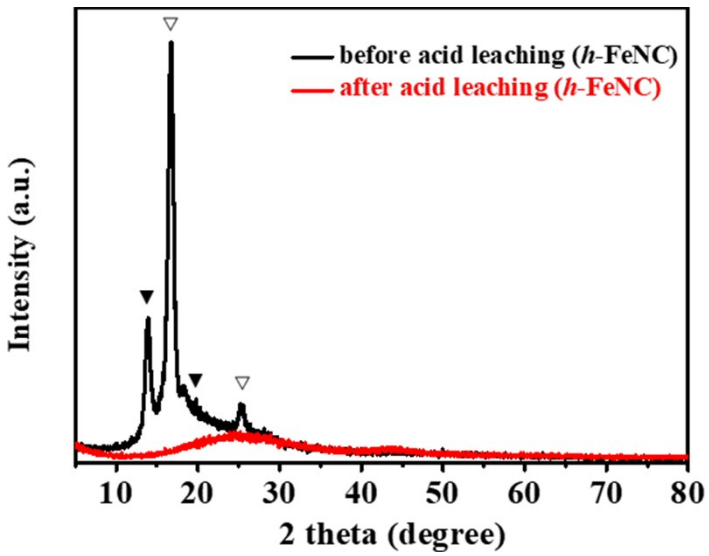


**Fig. S1** XRD test of *h*-FeNC with and without acid leaching.

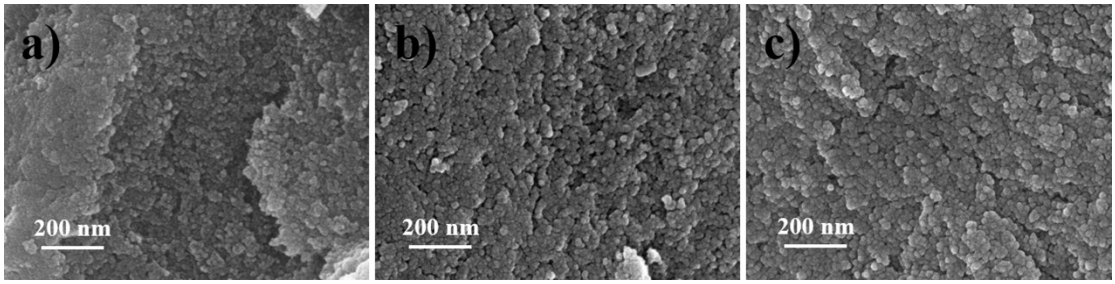


**Fig. S2** SEM of *p*-FeNC, *r*-FeNC and *c*-FeNC.

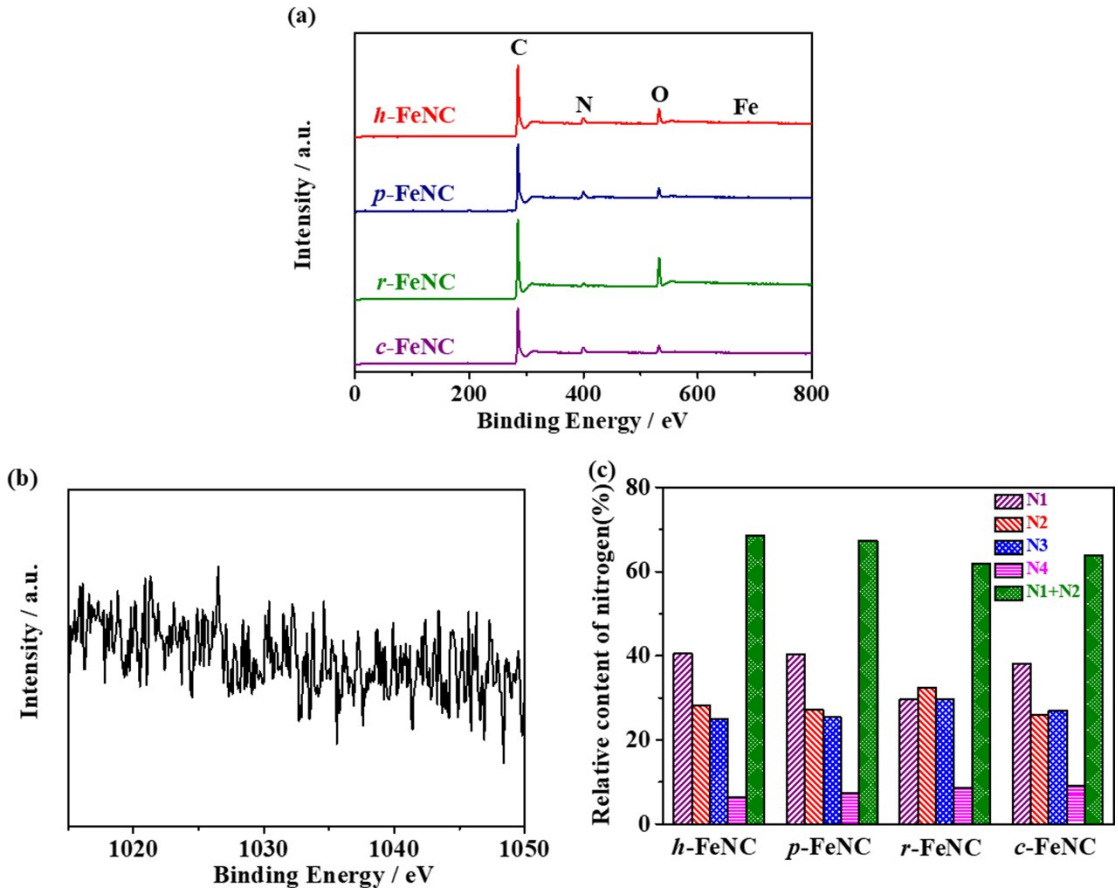


**Fig. S3** (a) Full XPS spectrum of *h*-FeNC, *p*-FeNC, *r*-FeNC and *c*-FeNC. (b) Zn 2p XPS spectrate of *h*-FeNC and (c) the ratio of different N species of *h*-FeNC, *p*-FeNC, *r*-FeNC and *c*-FeNC.

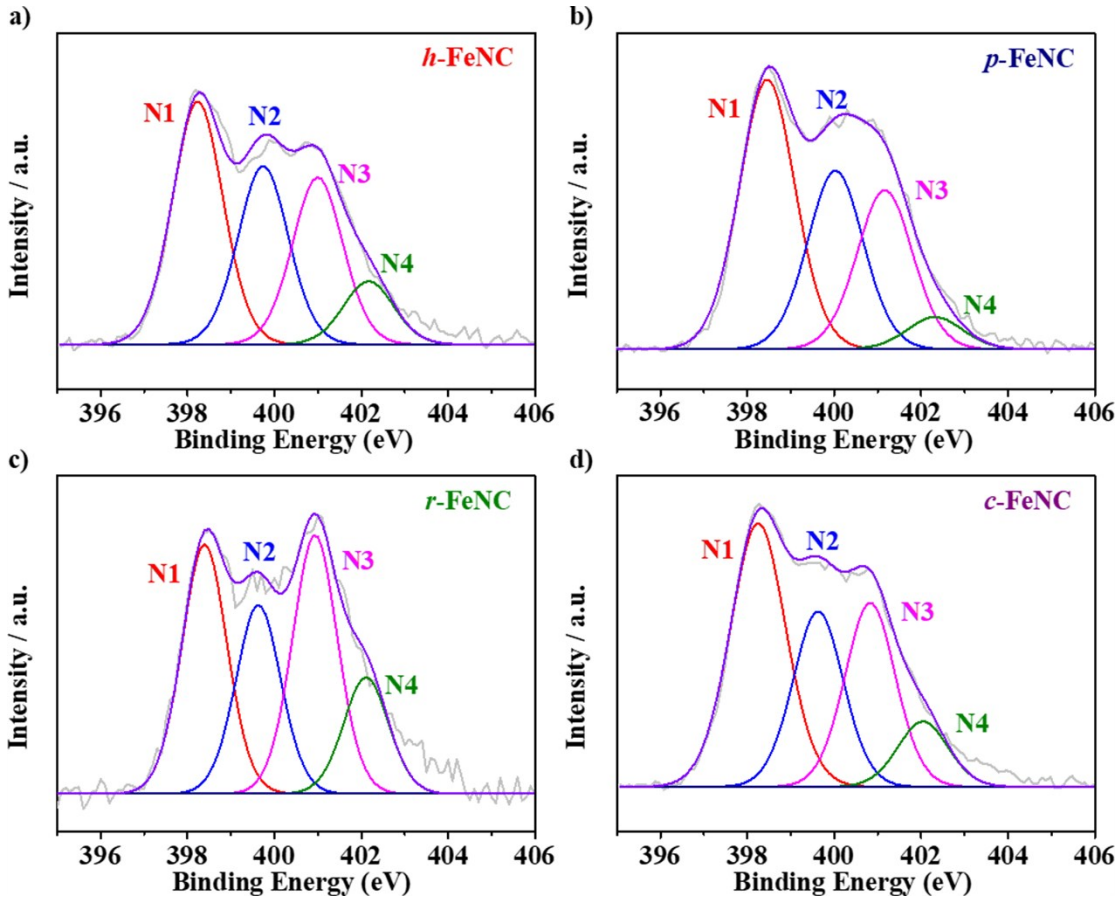


**Fig. S4** N1s XPS deconvolution results of *h*-FeNC, *p*-FeNC, *r*-FeNC and *c*-FeNC.

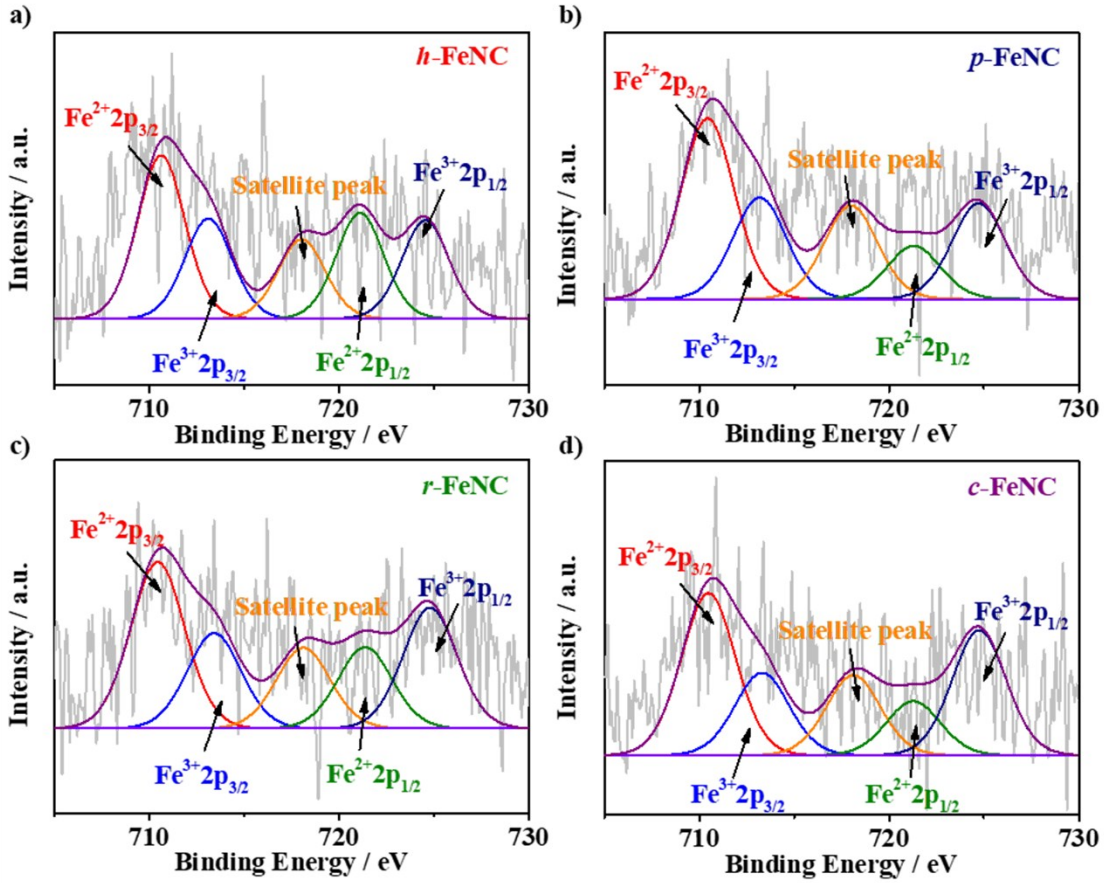


**Fig. S5** Fe 2p XPS deconvolution results of *h*-FeNC, *p*-FeNC, *r*-FeNC and *c*-FeNC.

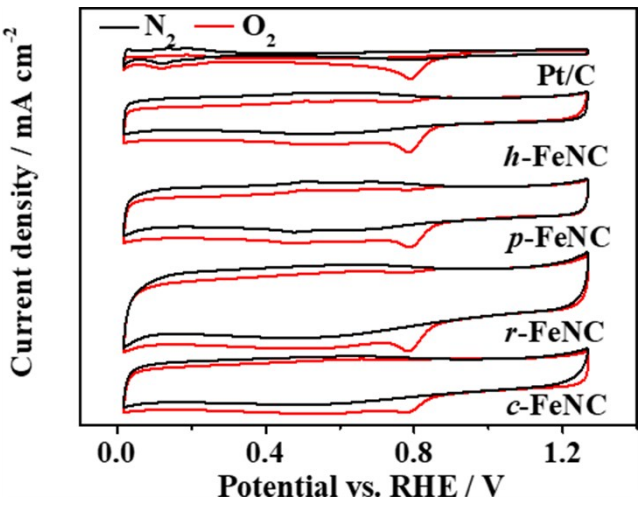


**Fig. S6** CVs of Pt/C, *h*-FeNC, *p*-FeNC, *r*-FeNC and *c*-FeNC in $N_2$- and $O_2$-saturated 0.1 M $HClO_4$ solution at a scan rate of 10 mV $s^{-1}$.

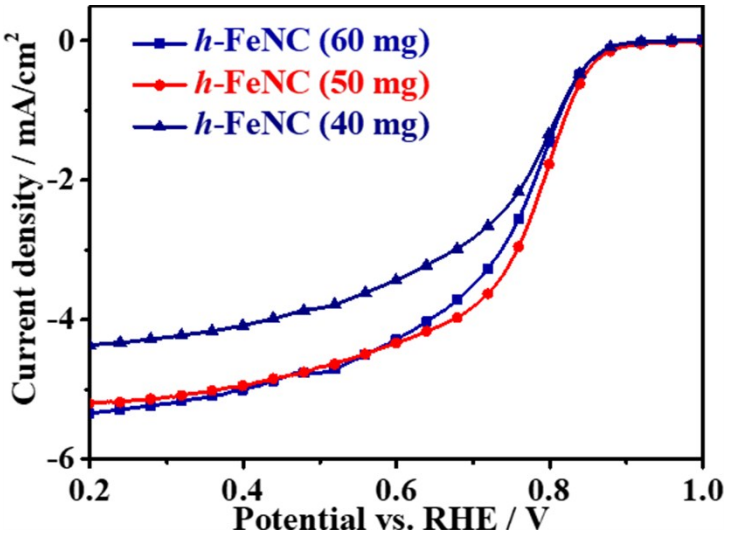


**Fig. S7** LSV of *h*-FeNC with different $Fe_2O_3$ content in 0.1 M $HClO_4$ solution at a scan rate of 10 mV $s^{-1}$.

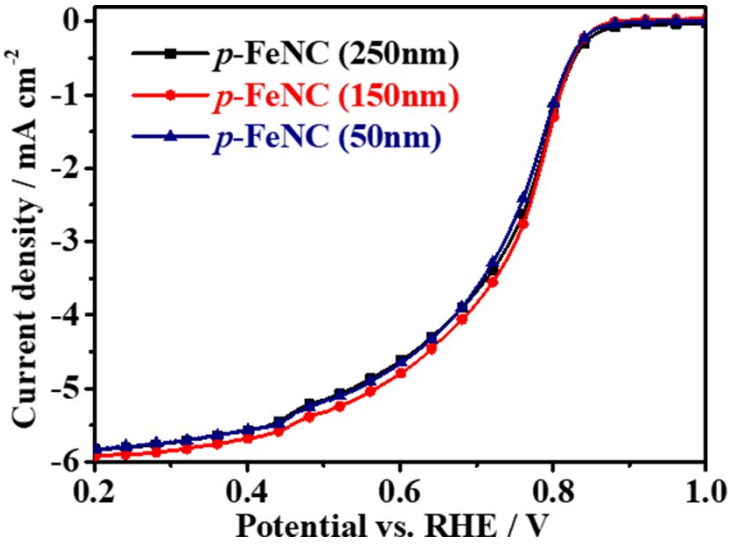


**Fig. S8** RDE polarization curves of *p*-FeNC (250 nm), *p*-FeNC (150 nm) and *p*-FeNC (50 nm) in $O_2$-saturated 0.1 M $HClO_4$ solution at 1600 rpm, with a scan rate of 10 mV $s^{-1}$.

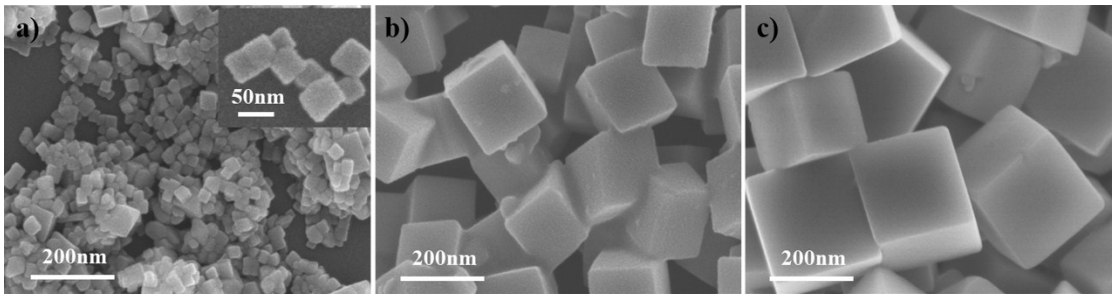


**Fig. S9** SEM of *p*-$Fe_2O_3$ with different sizes (a) 50 nm, (b) 150nm and (c) 250 nm.

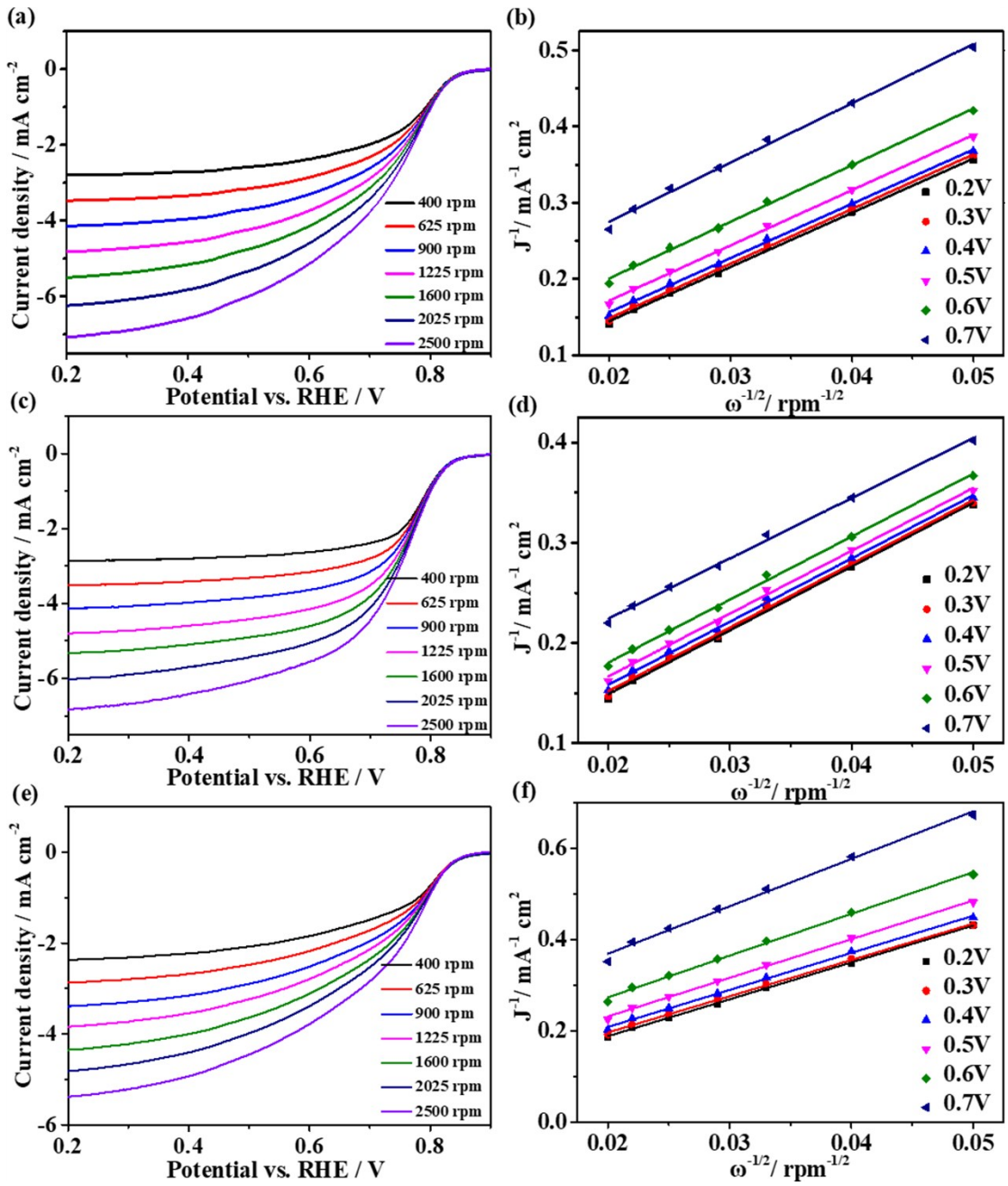


**Fig. S10** (a, c, e) LSV curves of *p*-FeNC, *r*-FeNC and *c*-FeNC at different rotating speeds with a scan rate of 10 mV $s^{-1}$ in $O_2$-saturated 0.1 M $HClO_4$ solution, respectively. (b, d, f) the corresponding Koutecky-Levich plots of *p*-FeNC, *r*-FeNC and *c*-FeNC, respectively.

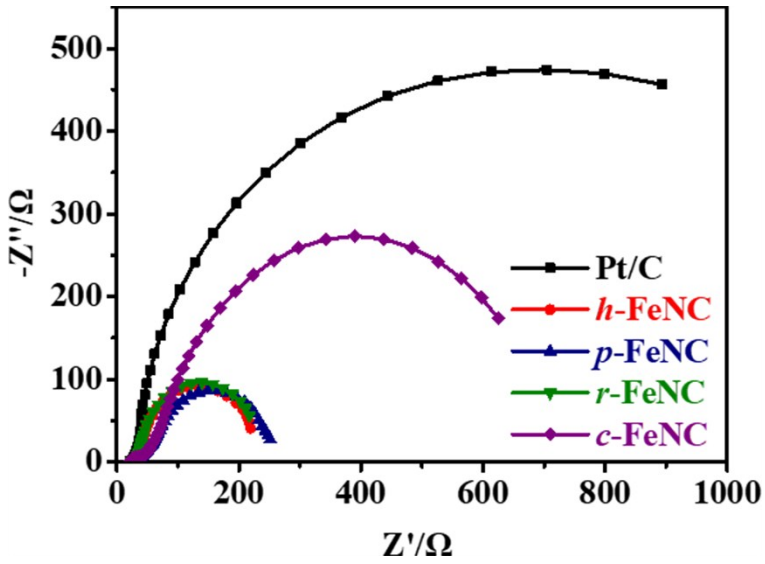


**Fig. S11** The electrochemical impedance spectra of Pt/C, *h*-FeNC, *p*-FeNC, *r*-FeNC and *c*-FeNC.

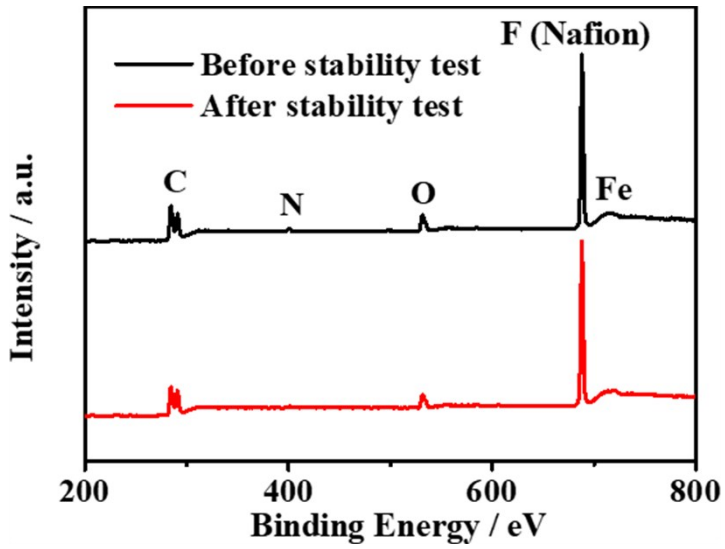


**Fig. S12** Full XPS spectrum of *h*-FeNC before and after stability test.

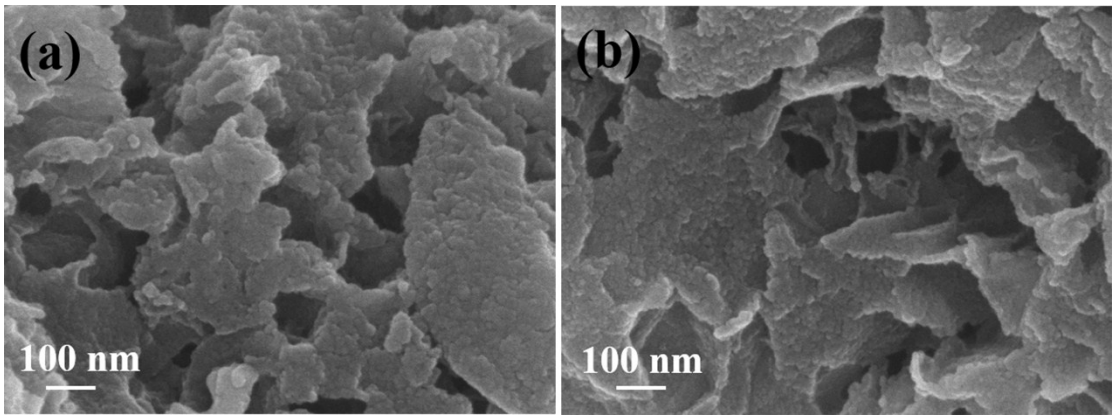


**Fig. S13** SEM of *h*-FeNC before and after stability test.

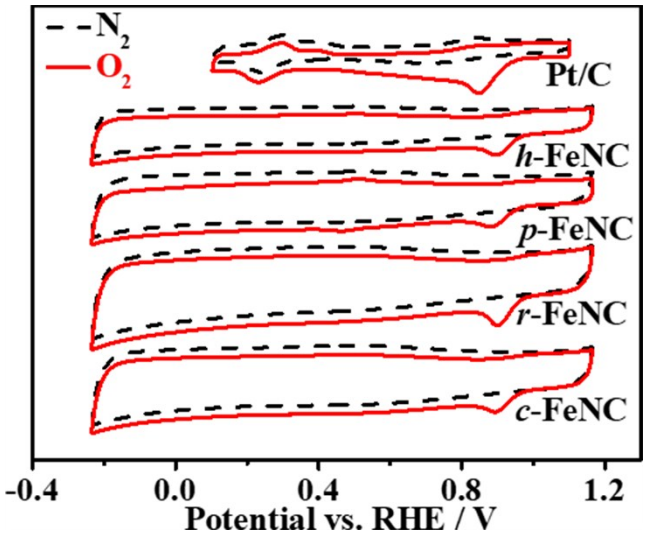


**Fig. S14** CVs of Pt/C, *h*-FeNC, *p*-FeNC, *r*-FeNC and *c*-FeNC in $N_2$- and $O_2$-saturated 0.1 M KOH solution at a scan rate of 10 mV $s^{-1}$.

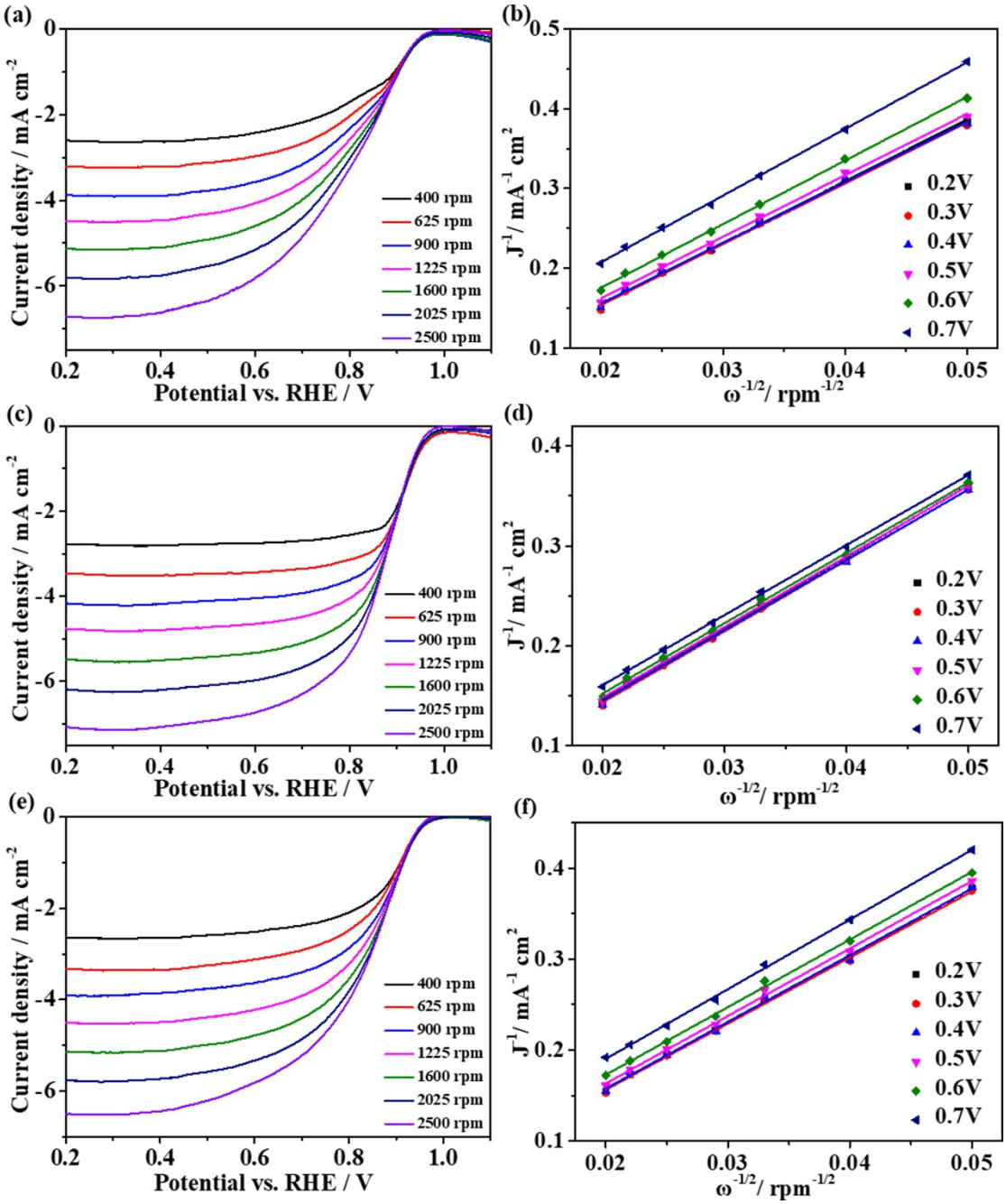


**Fig. S15** (a, c, e) LSV curves of *p*-FeNC, *r*-FeNC and *c*-FeNC at different rotating speeds with a scan rate of 10 mV $s^{-1}$ in $O_2$-saturated 0.1 M KOH solution, respectively. (b, d, f) the corresponding Koutecky-Levich plots of *p*-FeNC, *r*-FeNC and *c*-FeNC, respectively.

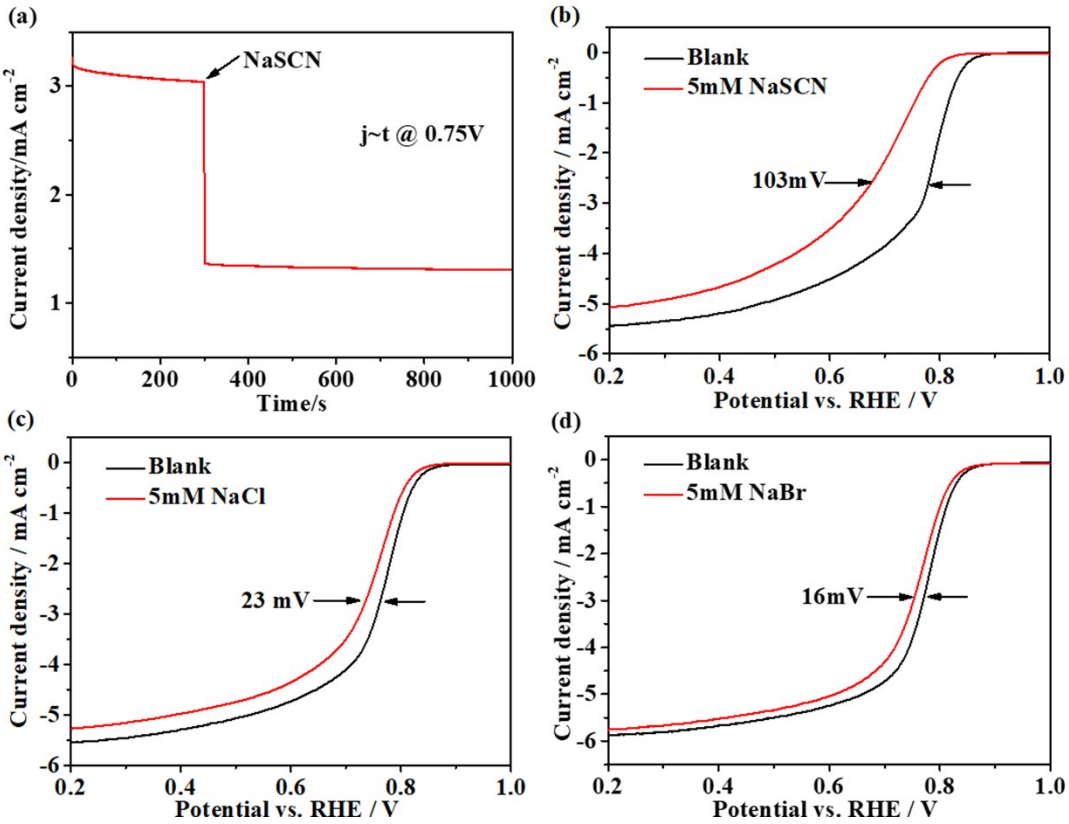


**Fig. S16** (a) Current-time (I-t) curves and (b) RDE results of *h*-FeNC in $O_2$-saturated 0.1 M $HClO_4$ solution (without and with $SCN^-$). (c, d) RDE results of *h*-FeNC in $O_2$-saturated 0.1 M $HClO_4$ solution (without and with $Cl^-$, without and with $Br^-$). All tests on a rotating disk electrode (1600 rpm) with a scan rate of 10 mV $s^{-1}$.

**Table S1** Nitrogen sorption analysis results of *h*-FeNC, *p*-FeNC, *r*-FeNC and *c*-FeNC.

| Sample | $S_{BET}$ ($m^2\ g^{-1}$) | $V_{tol}$ ($cm^3\ g^{-1}$) | $D_{av}$ (nm) |
|---|---|---|---|
| *h*-FeNC | 2454 | 1.9 | 3.4 |
| *p*-FeNC | 2248 | 1.7 | 3.3 |
| *r*-FeNC | 1934 | 1.6 | 3.2 |
| *c*-FeNC | 1864 | 1.6 | 3.2 |

**Table S2** The XPS atomic ratio of *h*-FeNC, *p*-FeNC, *r*-FeNC and *c*-FeNC.

| Sample | XPS atomic ratio (%) | | | | |
|---|---|---|---|---|---|
| | **N1** | **N2** | **N3** | **N4** | **N1+N2** |
| *h*-FeNC | 40.51 | 28.14 | 24.95 | 6.40 | 68.65 |
| *p*-FeNC | 40.22 | 27.17 | 25.36 | 7.25 | 67.39 |
| *r*-FeNC | 29.53 | 32.38 | 29.52 | 8.57 | 61.91 |
| *c*-FeNC | 38.04 | 25.84 | 26.97 | 9.15 | 63.88 |

**Table S3** The electrocatalytic activities of *h*-FeNC and some recently reported NMP catalysts for ORR in acidic media.

| Catalyst | Electrode rotation speed (rpm) | Half-wave Potential (mV) | Catalyst loading (mg $cm^{-2}$) | Reference |
|---|---|---|---|---|
| *h*-FeNC | 1600 | 777 | 0.4 | This work |
| Co-N-C | 1200 | 761 | 0.6 | S1 |
| FePPyC-900 | 1600 | 740 | 0.4 | S2 |
| $Fe_3C$/C-700 | 900 | 730 | 0.6 | S3 |
| PANI-Co-C | 900 | 750 | 0.6 | S4 |
| Fe-N-GC-900 | 1600 | 740 | 0.6 | S5 |
| Fe-Nx/HPC | 1600 | 760 | 0.2 | S6 |
| Fe-g-$C_3N_4$@C | 900 | 750 | 0.6 | S7 |
| FeNC-900 | 1600 | 720 | 0.6 | S8 |

**Table S4** The change of C, N, O and Fe content of *h*-FeNC before and after the stability test.

| Sample | XPS | | | |
|---|---|---|---|---|
| | △C/C (at %) | △N/N (at %) | △O/O (at %) | △Fe/Fe (at %) |
| *h*-FeNC | -0.71 | +6.41 | +2.43 | +1.20 |

**Table S5** The electrocatalytic activities of *h*-FeNC and some recently reported NMP catalysts for ORR in 0.1 M KOH solution.

| Catalyst | Electrode rotation speed (rpm) | Half-wave potential (mV) | Catalyst loading (mg $cm^{-2}$) | Reference |
|---|---|---|---|---|
| *h*-FeNC | 1600 | 883 | 0.4 | This work |
| NiCo/NLG-270 | 1600 | 820 | 0.4 | S9 |
| Co/N-CNTs | 1600 | 840 | 0.2 | S10 |
| Fe-N/C-800 | 1600 | 809 | 0.1 | S11 |
| PFA-Fe20-900-ALP | 1500 | 830 | 0.8 | S12 |
| Fe@Aza-PON | 1600 | 839 | 0.239 | S13 |
| Fe-Phen-N-800 | 1600 | 860 | 0.1 | S14 |
| Fc-F/Co@N-C800 | 1600 | 860 | 0.2 | S15 |
| NCNT/$Co_XMn_{1-X}O$ | 1600 | 840 | 0.2 | S16 |

## References


1 B. You, N. Jiang, M. Sheng, W. S. Drisdell, J. Yano and Y. Sun, *ACS Catal*., 2015, **5**, 7068-7076.
2 T. N. Tran, M. Y. Song, K. P. Singh, D. S. Yang and J. S. Yu, *J. Mater. Chem. A*, 2016, **4**, 8645-8657.
3 Y. Hu, J. O. Jensen, W. Zhang, L. N. Cleemann, W. Xing, N. J. Bjerrum and Q. Li, *Angew. Chem. Int. Ed*., 2014, **53**, 3675-3679.
4 G. Wu, K. L. More, C. M. Johnston and P. Zelenay, *Science*, 2011, **332**, 443-447.
5 A. Kong, X. Zhu, Z. Han, Y. Yu, Y. Zhang, B. Dong and Y. Shan, *ACS Catal*., 2014, **4**, 1793-1800.
6 Z. Zhang, X. Gao, M. Dou, J. Ji and F. Wang, *J. Mater. Chem. A*, 2017, **5**, 1526-1532.
7 M. Wang, W. Yang, H. Wang, C. Chen, Z. Zhou and S. Sun, *ACS Catal*., 2014, **4**, 3928-3936.
8 Q. Zuo, P. Zhao, W. Luo and G. Cheng, *Nanoscale*, 2016, **8**, 14271-14277.
9 X. Wang, J. Liu, Z. Liu, W. Wang, J. Luo, X. Han, X. Du, S. Qiao and J. Yang, *Adv. Mater*., 2018, **30**, 1800005.
10 Y. Liu, H. Jiang, Y. Zhu, X. Yang and C. Li, *J. Mater. Chem. A*, 2016, **4**, 1694-1701.
11 L. Lin, Q. Zhu and A. Xu, *J. Am. Chem. Soc*., 2014, **136**, 11027-11033.
12 L. C. P. Pérez, N. R. Sahraie, J. Melke, P. Elsässer, D. Teschner, X. Huang, R. Kraehnert, R. J. White, S. Enthaler, P. Strasser and A. Fischer, *Adv. Funct. Mater*., 2018, **28**, 1707551.
13 S. J. Kim, J. Mahmood, C. Kim, G. Han, S. W. Kim, S. M. Jung, G. Zhu, J. J. D. Yoreo, G. Kim and J. B. Baek, *J. Am. Chem. Soc*., 2018, **140**, 1737-1742.
14 Z. Yang, Z. Zhao, K. Liang, X. Zhou, C. Shen, Y. Liu, X. Wang and A. Xu, *J. Mater. Chem. A*, 2016, **4**, 19037-19044.
15 M. Tan, T. He, J. Liu, H. Wu, Q. Li, J. Zheng, Y. Wang, Z. Sun, S. Wang and Y. Zhang, *J. Mater. Chem. A*, 2018, **6**, 8227-8232.
16 X. Liu, M. Park, M. G. Kim, S. Gupta, X. Wang, G. Wu and J. Cho, *Nano Energy*, 2016, **20**, 315-325.